Title

In situ x-ray absorption spectroscopy study of hydrogen absorption by nickel-magnesium thin films

Journal

Physical Review B, 6708(8)

Authors

Farangis, B.
Nachimuthu, P.
Richardson, T.J.
et al.

Publication Date

2002-07-09

LBNL-51067
OM-477

Submitted to Physical Review B for publishing, July 11, 2002

In situ x-ray absorption spectroscopy study of hydrogen absorption by nickel-magnesium thin films

B. Farangis,[1] P. Nachimuthu,[2,3] T. J. Richardson,[1*] J. L. Slack,[1] R. C. C. Perera,[2] E. M. Gullikson,[2] D. W. Lindle,[3] and M. Rubin[1]

[1] *Environmental Energy Technologies Division*
[2] *Center for X-ray Optics, Materials Sciences Division*
Lawrence Berkeley National Laboratory
1 Cyclotron Road, Berkeley, CA 94720

[3] *Department of Chemistry*
University of Nevada,
Las Vegas, NV 89154

July 2002

This work was supported by the Assistant Secretary for Energy Efficiency and Renewable Energy, Office of Building Technology, State and Community Programs, Office of Building Research and Standards of the U.S. Department of Energy under Contract No. DE-AC03-76SF00098. The Advanced Light Source is operated by the Director, Office of Science, Office of Basic Energy Sciences, Division of Materials Science of US Department of Energy under Contract No. DE-AC03-76SF00098 at LBNL. Financial support from the National Science Foundation under contract Nevada-NSF-EPSCoR is gratefully acknowledged.

In situ x-ray absorption spectroscopy study of hydrogen absorption by nickel-magnesium thin films

B. Farangis, *****P. Nachimuthu, T. J. Richardson,[*] J. L. Slack, R. C. C. Perera,
E. M. Gullikson, M. Rubin
Lawrence Berkeley National Laboratory

D. W. Lindle
*University of Nevada

Structural and electronic properties of co-sputtered Ni-Mg thin films with varying Ni to Mg ratio were studied by *in-situ* x-ray absorption spectroscopy in the Ni L-edge and Mg K-edge regions. Co-deposition of the metals led to increased disorder and decreased coordination around Ni and Mg compared to pure metal films. Exposure of the metallic films to hydrogen resulted in formation of hydrides and increased disorder. The presence of hydrogen as a near neighbor around Mg caused a drastic reduction in the intensities of multiple scattering resonances at higher energies. The optical switching behavior and changes in the x-ray spectra varied with Ni to Mg atomic ratio. Pure Mg films with Pd overlayers were converted to MgH_2: the H atoms occupy regular sites as in bulk MgH_2. Although optical switching was slow in the absence of Ni, the amount of H_2 absorption was large. Incorporation of Ni in Mg films led to an increase in the speed of optical switching but decreased maximum transparency. Significant shifts in the Ni L_3 and L_2 peaks are consistent with strong interaction with hydrogen in the mixed films.

*tjrichardson@lbl.gov
PACS: 61.10.Ht, 78.20.-e, 78.66.-w, 82.30.-b

I. INTRODUCTION

Switchable mirrors exhibiting variable optical, mechanical and electrical properties due to uptake and removal of hydrogen were discovered by Huiberts *et al.*[1] They have significant potential for applications in light and heat regulation, display devices, and optical communication systems. The first generation of switchable mirrors was based on rare earth metals which undergo a reversible metal-insulator transition when thin films coated with palladium are exposed to H_2.[2] Van der Sluis *et al.*[3] reported that incorporation of magnesium increased the transparency of lanthanide hydride films. The larger optical band gap (3.4 eV) for $Gd_{0.5}Mg_{0.5}H_{2.5}$ makes this switchable mirror colorless in contrast to reddish GdH_3. Recently Richardson *et al.*[4,5] reported switchable mirror effects in thin films of Mg and 3d transition metals (Ni, Mn, Fe, and Co). These are potentially more cost effective since they do not require the expensive and reactive rare earth metals.

A recent report[6] on the hydrogenation of 200 nm thick Mg films with Pd over-layers by H_2 gas at 0.1 MPa and 100° C showed that magnesium hydride is formed, with H_2 loading ranging from 2.9 to 6.6 wt.%. After 24 h, transparent magnesium hydride was obtained.[7] The temperature required for dehydrogenation decreased with decreasing degree of crystallization. Heating the hydride film led to the formation of nano-structured magnesium. H_2 absorption leads to lattice expansion and structural rearrangements, which modify the electronic properties of the films.

Near-edge x-ray absorption fine structure (NEXAFS) and extended x-ray absorption fine structure (EXAFS) are powerful tools for understanding the electronic and structural properties of thin films.[8-10] These techniques are element-specific and capable of probing the short to medium range structure around an absorbing atom. Among the experimental techniques employed in determining the valence states of atoms in solids, NEXAFS plays a crucial role due to its simplicity and universal applicability. EXAFS is sensitive to the local structure around an atom, and is especially useful in studying amorphous materials.

X-ray absorption spectroscopy (XAS) and X-ray magnetic circular dichroism (XMCD) are used to study the electronic and magnetic properties of *3d* elements. Theoretical and experimental studies have shown that the band structure of bulk Ni is

different from that of Ni thin films grown on Cu and Co.[11-14] This results in different electronic and magnetic properties. The line shapes of XAS and XMCD spectra can change dramatically for varying film thickness due to electron transfer and hybridization at the interface or due to 3*d* electron correlation effects.[15] Srivastava *et al.*[16] have shown that the thickness dependent density of 3*d* holes for Ni thin films grown on Cu (001) gives rise to a modified XAS line shape. Therefore a detailed analysis of Ni $L_{2,3}$ edges (which is a direct measure of unoccupied d states) and Mg K-edge are a useful approach to study the electronic structure of our samples in the metallic and hydride state.

Here we report an investigation of the structural and electronic properties of Ni-Mg thin films with varying Ni to Mg atomic ratio using *in-situ* x-ray absorption spectroscopy. The mirror-like metallic Ni-Mg thin films become optically transparent due to H_2 absorption. We followed the hydrogenation processes by recording x-ray absorption spectra at both the Mg K and Ni L-edges.

Experimental Procedure

Sample preparation

Ni-Mg films for the present study were prepared by dc magnetron co-sputtering from 50 mm Ni and Mg (99.98%) targets inclined 22.5° from normal onto silicon nitride membrane substrates (Silson Ltd., Northampton, UK), which were mounted sequentially on a glass plate to obtain different Ni to Mg atomic ratios. The base pressure was 1.4×10^{-7} Torr, process pressure 2 mTorr, Ni power 24 W, Mg power 47 W, target-to-substrate distance 7.5 cm. Deposition rates ranged from 0.33 to 0.55 nm/s, depending on location of the substrate. Palladium was deposited over all Ni-Mg films to protect them from air oxidation and to promote absorption of hydrogen. The Pd over-layer was applied at 10 mTorr, Pd power 12.4 W, with deposition rate 0.16 nm/s. Film thicknesses and compositions were measured by stylus profilometry and Rutherford back scattering (RBS). Mg_2Ni (containing 20% excess Mg) was purchased from Ergenics, Inc., (Ringwood, NJ) and MgH_2 (nominal purity 90 %, remainder Mg) from Aldrich Chemical Co, (Milwaukee, WI). Powder x-ray diffraction patterns (xrd) for these compounds confirmed their bulk compositions and purity.

X-ray absorption measurements

The x-ray absorption spectra were measured at beamlines 6.3.1 and 6.3.2 at the Advanced Light Source, Lawrence Berkeley National Laboratory.[17] During the measurements, the synchrotron was typically operated at 1.9 GeV between 200 and 400 mA. The spectra were recorded at the Mg K and Ni L absorption edges in the bulk-sensitive transmission detection mode, in an atmosphere of He using a 4.6x4.6 mm photodiode detector (Hamamatsu, G1127-02). Hydrogenation of the films was achieved by purging with 4 % H_2 in He. The spectra for reference materials Mg_2Ni and MgH_2 were measured by total fluorescence yield (TFY) using a 28x28 mm windowless detector (Hamamatsu, S3584-06). The resolution at the Mg K and Ni L-edges was better than 1.5 and 1.0 eV, respectively. The photon energy was calibrated to the first inflection point of the Ni L_3 edge at 852.7 eV and Mg K edge at 1303.0 eV.[18] After calibration, the spectra were normalized to the absorption edge jumps.[8] All measurements were performed at room temperature.

Results and Discussion

Previous work[3] on Ni-Mg thin films showed that the Ni to Mg atomic ratio and the film thickness are factors in determining the speed at which switching takes place between the metallic state and the transparent hydride state. The freshly sputtered films were amorphous by xrd, showing only weak reflections due to Pd. Co-deposition from offset sources yielded films with position-dependent Ni–Mg atomic ratio and thickness (Table I). They absorbed hydrogen rapidly and reached maximum transparency within a few minutes. When samples were annealed at 125 ^oC in dry nitrogen, xrd reflections due to Mg_2Ni, Mg, and Mg_6Pd developed. The annealed films did not take up H_2 readily.

Ni $L_{3,2}$-edge NEXAFS

Ni $L_{3,2}$-edge x-ray absorption spectra measured in transmission mode in He and in 4 % H_2 (balance He) for a pure Ni film and two Ni-Mg films are shown in Fig. 1. The spectrum for Mg_2Ni powder measured by total fluorescence yield is included for comparison. The transitions denoted as L_3 and L_2, at ~853.5 eV and ~870.8 eV, are from Ni $2p_{3/2}$ and $2p_{1/2}$ to 3d final states, respectively.[15,18,19] Satellites at ~3 eV and ~6 eV above the L_3-edge are seen in all the spectra. The intensity of 6 eV satellite for Ni-Mg

films and Mg_2Ni are reduced by a factor of five compared to pure Ni film. Recently Dhesi *et al.*[19,20] assigned these satellites to transitions to triplet (3 eV) and singlet (6 eV) states of the final $2p^5 3d^9$ configuration, split by the core-valence exchange interaction (multiplet effects). The singlet state can be reached from the triplet $3d^8$ initial state by spin-flip transitions due to the 2p spin-orbit interaction. More recently, Nesvizhskii *et al.*[21] based on one-electron multiple scattering and atomic multiplet calculations claimed that the effect of spin-flip transition is negligible and hence the 6 eV satellite is predominantly due to multiple scattering effect, but that the multiplet explanation of Dhesi *et al.*[19,20] is applicable for the 3 eV satellite. The reduced intensity for the 6 eV satellite observed for Ni-Mg films in the present study is therefore attributed to a decreased multiple scattering due to the presence of Mg and the amorphous character of the films.

Spectra were recorded at both Mg K and Ni L-edges during hydrogen loading of films. Ni $L_{3,2}$ spectra of $Ni_{0.24}Mg_{0.76}H_x$ at different exposure times are presented in Figure 2. The spectrum denoted as 'end of hydrogenation' was recorded after exposure to hydrogen for 24 h. Further exposure produced no changes in the spectrum. H_2 absorption led to a shift towards higher energy and an enhancement in intensity. The extent of both effects depended upon exposure time and Ni:Mg ratio. The time required to reach saturation, corresponding to the optical switching from mirror state to maximum transparency, also depended on the film thickness. Figure 3 shows Ni $L_{3,2}$ spectra for a $Ni_{0.24}Mg_{0.76}$ film as-deposited, fully hydrogenated and dehydrogenated by exposure to air for 24 h. The hydrogen is apparently not completely removed under these conditions.

The full width at half maximum (FWHM) and integrated area for each band was obtained by fitting the Ni L-edge spectra with Gaussian functions. To exclude the edge jump, asymmetric double sigmoidal functions were also included in the fits. The results, along with branching ratios $\beta_R = A_3/(A_3+A_2)$, total integrated intensity (A_3+A_2), and intensity ratio (A_3/A_2), are given in Table II. It has been shown that, due to changes in the final state energies, Ni $L_{3,2}$ transitions shift towards higher energy by about 1 eV for each unit increase in oxidation state.[22-25] Since the integrated intensity (A_3+A_2) is a ground state property, it is a quantitative and a direct measure of 3d shell vacancies (n_h).[16,19,22,24] Further, the initial state 3d spin-orbit coupling and the overlap of 2p and 3d wave

functions, the so called multiplet effects, are said to affect the branching ratio (β_R).[26,27] Another report, however, maintains that multiplet effects dominate all other interactions.[28] Recent reports demonstrate that one can distinguish the nature of spin states, *viz.*, low spin and high spin for a given oxidation state of Ni, based on the branching ratios (β_R) of $L_{3,2}$-edges.[23-25]

In the present study, the energy separation (E_3-E_2) between the L_3 and L_2-edges, which is due to 2p spin-orbital splitting, for all the samples is found to be ~17.3 eV in accordance with earlier reports.[15,16,19] The transition energies (E) for both $L_{3,2}$-edges of a Ni film and Ni-Mg films in the metallic state show a small trend towards higher energy from pure Ni film to very Mg-rich ($Ni_{0.13}Mg_{0.87}$). The spectral profile and branching ratio for pure Ni film are in good agreement with the pervious reports on bulk Ni metal and for Ni films grown on Cu(001) and Co/Cu(001).[16,19] The Ni film was therefore utilized as a reference for Ni-Mg films. The total integrated intensity (A_3+A_2) is smaller and, the β_R and A_3/A_2 are larger for Ni-Mg than for Ni (Table II). These results suggest that the addition of Mg produces structural changes and modification of Ni electronic states. Similar results were reported for Ni film on Cu(001) and Co/Cu(001) due to charge transfer to Ni.[16,19]

Hydrogen uptake by Ni-Mg films caused the transition energies for both $L_{3,2}$-edges to shift significantly towards higher energy, by ~2.3 eV for $Ni_{0.33}Mg_{0.67}$ and ~2.6 eV for $Ni_{0.13}Mg_{0.87}$. The total integrated intensity and FWHM also increase. The values for β_R and A_3/A_2 are comparable to those for the Ni film. In general, the effective charge transfer from metal to hydrogen is reported to be less for metal hydrides than for halides, oxides, etc. where the charge transfer is much greater.[29,30] This is supported by the values of β_R and A_3/A_2 for Ni-Mg films in the hydride state, which are comparable to those for the Ni film, indicating that although Ni is in a higher oxidation state, the effective charge transfer in the hydride is less than in the metal. The values of β_R suggest that Ni in hydrided Ni-Mg films is in a high-spin state.[23-25] Hydriding also leads to the creation of non-equivalent Ni sites, which result in larger FWHMs.

Mg K-edge NEXAFS

Mg K near-edge transmission mode spectra of a pure Mg film (270 nm) and two extreme compositions of Ni-Mg films in He and in 4 % H_2 are shown in Fig. 4. The Mg K-edge is shifted to lower energy for Ni-Mg films in the metallic state (1302.2 eV) compared to pure Mg film (1303.0 eV). The intensity of the spectral profile at 1304.5 eV decreases for Ni rich $Ni_{0.33}Mg_{0.67}$ film when compared to Mg rich $Ni_{0.33}Mg_{0.67}$ and pure Mg films. Spectra reported for magnesium halides, magnesium oxide, and Mg in minerals and disordered systems show not only a sharp near-edge peak at ~1310 eV due to the 1s to 3p transition whose intensity depends on the degeneracy of the 3p states but also this feature shifts towards higher energy with increasing coordination around Mg.[31-35] In the present study, the transition at 1304.5 eV in pure Mg and Ni-Mg films is assigned to Mg 1s to 3p. The edge shift towards lower energy and reduction in the intensity of the peak with increasing nickel content suggest that the coordination around Mg decreases, resulting in lowering of 3p degeneracy.

The NEXAFS total fluorescence yield (TFY) spectra for the pure Mg film (270 nm), for Mg_2Ni and MgH_2 powder samples, and a transmission mode spectrum of a thin Mg film (45 nm) in the presence of He and 4 % H_2 are shown in Figure 5. The similarity in the spectral profiles and edge positions for Mg_2Ni and the $Ni_{0.33}Mg_{0.67}$ film are consistent with Mg-Ni bonding in the film. The Mg K-edge TFY spectrum for the pure Mg film (270 nm) differs from the transmission mode spectrum (Figs. 4 and 5). Transmission measurements are bulk-sensitive, while TFY probes only to ca. 100 nm in depth. The TFY spectrum for the Mg film reflects both pure Mg and the Mg-Pd interface region. Comparison with the transmission spectrum of a thinner (45 nm) Mg film confirms the presence of different surface and bulk compositions.

The Mg K-edge spectra shifted towards higher energy by ~2.2 and ~2.9 eV for $Ni_{0.33}Mg_{0.67}$ and $Ni_{0.13}Mg_{0.87}$, respectively, when hydrogen is introduced. In addition, the transitions at higher energies due to multiple scattering resonances were significantly reduced by the presence of hydrogen, which scatters weakly due to its low mass.[36,37] The spectrum of the thick Mg film showed no significant changes on exposure to H_2 for 2 h, consistent with previous observations of very slow diffusion of hydrogen in relatively thick Mg films.[29] The thin Mg film, however exhibited a 3.5 eV shift following overnight

soaking in 4 % H_2 at room temperature. This is consistent with optical properties of Mg film with Pd overlayer, which show that an increase in Mg thickness decreases the optical response to hydrogen exposure.[38] The Mg K-edge TFY spectrum for bulk MgH_2 also shows a shift of ~2.3 eV towards higher energy compared to the Mg film, consistent with the presence of divalent Mg.

Magnesium K-Edge EXAFS

EXAFS data were analyzed using a background-subtraction method[39-43] with optimization of the low *r* portion of the EXAFS, followed by Fourier transformation to *r* space. The normalized spectra of the 270 nm Mg film and two Ni-Mg films are shown in Figure 6. The magnitude of the oscillations decreased with increasing nickel concentration in as-deposited Ni-Mg films due to disruption of the Mg structure. In the hydride state only very weak EXAFS oscillations were observed irrespective of Ni content. Comparison of EXAFS for Ni-Mg films in the hydride and metallic states with bulk MgH_2 and Mg_2Ni (Fig. 7) suggests that more of the magnesium in the $Ni_{0.13}Mg_{0.87}$ film is hydrided than in the $Ni_{0.33}Mg_{0.67}$ film, where unreacted Mg_2Ni remains. To get more insight into the structural properties of Ni-Mg thin films, detailed analyses of the experimental EXAFS spectra were conducted by theoretical fits.

Scattering amplitudes and phase shift functions of the Mg-Mg, Mg-Ni, and Mg-O pairs in Mg, Mg_2Ni and MgO were calculated using the program FEFF (7.02).[40,41] The FEFFIT (2.5*d*),[42] which is based on a nonlinear least squares technique was used to fit the experimental *r* space EXAFS data. Phase-corrected Fourier transforms of $\chi(k)$ to *r* space with a k^2 weighting factor and a Hanning window function ($Dk1$ and $Dk2$=0.1) were performed using values of K_{min}, K_{max}, r_{min}, and r_{min} of 1.8 $Å^{-1}$, 5.6 $Å^{-1}$, 2.1 Å and 5.1 Å, respectively. The value of the passive electron reduction factor (S_0^2)[43] was deduced from the spectrum of MgO and used for fitting Ni-Mg film spectra.

The Fourier transformed k^2–weighted Mg K-edge EXAFS intensities for Ni-Mg films in their metallic states are presented in Figure 8 along with theoretical fits. Figure 9 shows the fitting results in k space. The resultant structural parameters, coordination number (N), bond distance (R) and Debye–Waller factor (σ^2) for Mg, $Ni_{0.13}Mg_{0.87}$ and $Ni_{0.33}Mg_{0.67}$ are given in Table III. Attempts were made to fit the data using Mg-Mg (first

and second shell), Mg-Ni and Mg-O interactions. No significant contributions from Mg-Ni and Mg-O were found. There is a decrease in amplitude of the Fourier-transformed intensity on the addition of nickel. The nearest neighbor and next nearest neighbor Mg-Mg shells experience a decrease in mean square relative displacement (MSRD) with increasing nickel concentration. Although the Ni-Mg films are amorphous by XRD, there is microscopic ordering up to the second shell (~4.5 Å), despite decreased coordination numbers and increases disorder with increasing Ni concentration.

Attempts to fit the EXAFS data for Ni-Mg films in the hydride states failed due to high signal to noise ratios and weak EXAFS oscillations due to the presence of hydrogen as nearest neighbor. The weak EXAFS oscillations in k space for Ni-Mg films in hydride state were therefore compared with reference materials MgH_2 and Mg_2Ni (Fig. 10).

The hydrided 45 nm Mg film shows the features similar to those in bulk MgH_2.[6,7] Hydrided Ni-Mg films, however, do not resemble bulk MgH_2. Instead, $Ni_{0.13}Mg_{0.87}$ and $Ni_{0.33}Mg_{0.67}$ in both metallic and hydrides state look more like Mg_2Ni. This suggests that the Ni-Mg films contain some Mg_2Ni, which dominates the Mg EXAFS spectrum and that this phase persists even when the free magnesium is converted to its hydride. These results are also consistent with the lower transparency of films with higher Ni content. A relatively small amount of Ni (~10 mol %) is sufficient to facilitate absorption of H_2.

Conclusions

The co-sputtered Ni–Mg films were amorphous. The presence of nickel led to increased disorder and decreased coordination around both Ni and Mg compared to pure metal films. Introducing H_2 into Ni-Mg films resulted in the formation of Mg-Ni and Mg hydrides, with significant positive edge shifts. The presence of hydrogen as a near neighbor around Mg produced a drastic reduction in the intensities of multiple scattering resonances at higher energies. The extent of hydriding depended on the Ni-Mg ratio. A thin pure Mg film also was converted to MgH_2. Although the absorption was much slower without nickel, the extent of hydriding was greater. Addition of Ni led to an increase in optical switching speed, a decrease in maximum optical transparency, and a decrease in Mg utilization, probably due to the presence of unreacted Mg_2Ni. Opimization of switching speed and desired transmittance and reflectance ranges requires adjustment both of the Ni-Mg ratio and film thickness.

Acknowledgements

This work was supported by the Assistant Secretary for Energy Efficiency and Renewable Energy, Office of Building Technology, State and Community Programs, Office of Building Research and Standards of the U.S. Department of Energy under Contract No. DE-AC03-76SF00098. The Advanced Light Source is operated by the Director, Office of Science, Office of Basic Energy Sciences, Division of Materials Science of US Department of Energy under Contract No. DE-AC03-76SF00098 at LBNL. Financial support from the National Science Foundation under contract Nevada-NSF-EPSCoR is gratefully acknowledged.

References

[1]J. N. Huiberts, R. Griessen, J. H. Rector, R. J. Wijngaarden, J. P. Dekker, D. G. de Groot, and N. J. Koeman, Nature (London) **380**, 231 (1996).

[2]R. Griessen, Europhysics News **32**, 40 (2001).

[3]P. van der Sluis, M. Ouwerkerk, and P. A. Duine, Appl. Phys. Lett. **70**, 3356 (1997).

[4]T. J. Richardson, J. L. Slack, R. D. Armitage, R. Kostecki, B. Farangis, and M. D. Rubin, Appl. Phys. Lett. **78**, 3047 (2001).

[5]T. J. Richardson, J. L. Slack, B. Farangis, and M. D. Rubin, Appl. Phys. Lett. **80**, 1349 (2002).

[6]K. Higuchi , H. Kajioka , K. Toiyama , H. Fujii , S. Orimo , and Y. Kikuchi, J. Alloys and Compds. **293–5**, 484 (1999).

[7]K. Yamamoto , K. Higuchi , H. Kajioka , H. Sumida , S. Orimo , and H. Fujii, J. Alloys and Compds. **330–2**, 352 (2002).

[8]J. Stöhr, *NEXAFS Spectroscopy,* (Springer, New York, 1992),

[9]J. G. Chen, Surf. Sci. Rep. **30**, 1 (1997).

[10]F. M. F. de Groot, Chem. Rev. **101**, 1779 (2001).

[11]D. Wang, A. J. Freeman, and H. Krakauer, Phys. Rev. B **26**, 1340 (1982).

[12]J. Tersoff and L. M. Falicov, Phys. Rev. B **26**, 6186 (1982).

[13]O. Eriksson, A. M. Boring, R. C. Albers, G. W. Fernando, and B. R. Copper, Phys. Rev. B **45**, 2868 (1992).

[14]O. Hjortstam, J. Trygg, J. M. Wills, B. Johansson, and O. Eriksson, Phys. Rev. B **53**, 9204 (1996).

[15]S. S. Dhesi, E. Dudzik, H. A. Dürr, G. van der Lann, and N. B. Brookes, J. Appl. Phys. **87**, 5466 (2000).

[16]P. Srivastava, N. Haack, H. Wende, R. Chauvistré, and K. Baberschke, Phys. Rev. B **56**, R4398 (1997).

[17]J. H. Underwood and E. M. Gullikson, J. Eelctron Spectrosc. Relat. Phenom. **92**, 265 (1998).

[18]X-ray Data Booklet, LBNL/PUB490 Rev. 2 (2001).

[19]S. S. Dhesi, H. A. Dürr, G. van der Lann, E. Dudzik, and N. B. Brookes, Phys. Rev. B **60**, 12852 (1999).

[20]S. S. Dhesi, E. Dudzik, H. A. Dürr, N. B. Brookes, and G. van der Laan, Surf. Sci. **454-6**, 930 (2000).

[21]A. I. Nesvizhskii, A. L. Ankudinov, J. J. Rehr, and K. Baberschke Phys. Rev. B **62**, 15295 (2000).

[22]H. Wang, P. Ge, C. G. Riordan, S. Brooker, C. G. Woomer, T. Collins, C. A. Melendres, O. Graudejus, N. Bartlett, and S. P. Cramer, J. Phys. Chem. B **102**, 8343 (1998).

[23]H. Wang, C. Y. Ralston, D. S. Patil, R. M. Jones, W. Gu, M. Verhagen, M. Adams, P. Ge, C. Riordan, C. A. Marganian, P. Mascharak, J. Kovacs, C. G. Miller, T. J. Collins, S. Brooker, P. D. Croucher, K. Wang, E. I. Stiefel, and S. P. Cramer, J. Am. Chem. Soc. **122**, 10 544 (2000).

[24]H. Wang, D. S. Patil, W. Gu, L. Jacquamet, S. Friedrich, T. Funk, and S. P. Cramer, J. Electron Spectrosc. Relat. Phenom. **114–6**, 855 (2001).

[25]C. Y. Ralston, H. Wang, S. W. Ragsdale, M. Kumar, N. J. Spangler, P. W. Ludden, W. Gu, R. M. Jones, D. S. Patil, and S. P. Cramer, J. Am. Chem. Soc. **122**, 10553 (2000).

[26]B. T. Thole and G. van der Lann, Phys. Rev. B **38**, 3158 (1988).

[27]G. van der Lann and B. T. Thole, Phys. Rev. Lett. **60**, 1977 (1988).

[28]F. M. F. de Groot, Physica B **208-9**, 15 (1995).

[29]M. Gupta and L. Schlapbach, *Hydrogen in Intermetallic Compounds I*, edited by L. Schlapbach (Springer, Berlin, 1988), Chap. 6.

[30]R. Yu and P. K. Lam, Phys. Rev. B **37**, 8730 (1988).

[31]S. Naoé, T. Murata, and T. Matsukawa, Physica B **158**, 615 (1989).

[32]T. Yoshida, T. Tanaka, H. Yoshida, T. Funabiki, and S. Yoshida, J. Phys. Chem. **100**, 2302 (1996).

[33]H. Aritani, T. Tanaka, T. Funabiki, S. Yoshida, M. Kudo, and S. Hasegawa, J. Phys. Chem. **100**, 5440 (1996).

[34]H. Aritani, H. Yamada, T. Nishio, T. Shiono, S. Imamura, M. Kudo, S. Hasegawa, T. Tanaka, and S. Yoshida, J. Phys. Chem. **104**, 10 133 (2000).

[35]Ph. Ildefonse, G. Calas, A. M. Flank, and P. Lagarde, Nucl. Instr. and Meth. in Phys. Res. B **97**, 172 (1995).

[36]R R. G. Agostino, G. Liberti, V. Formoso, E. Colavita, A. Züttel, C. Nützenadel, L. Schlapbach A. Santaniello, and C. Gauthier, Phys. Rev. B **61**, 13 647 (2000).

[37]B. Lengeler, Phys. Rev. Lett. **53**, 74 (1984).

[38]T. J. Richardson *et al.*, unpublished.

[39]M. Newville, P. Livins, Y. Yacoby, J. J. Rehr, and E. A. Stern, Phys. Rev. B **47**, 14126 (1993).

[40]A. L. Ankudinov and J. J. Rehr, Phys. Rev. B **56**, R1712 (1997).

[41]A. L. Ankudinov, Ph.D. thesis, University of Washington, 1996.

[42]E. A. Stern, M. Newville, B. D. Ravel, Y. Yacoby, and D. Haskel, Physica B **208-9**, 117 (1995).

[43]E. A. Stern and S. M. Heald, in *Handbook on Synchrotron Radiation*, edited by E. E. Koch (North-Holland, New York, 1983), Vol. 1.

Table I. Ni-Mg Film and Pd over-layer thicknesses and compositions.

Sample	Film thickness (nm)	Pd over-layer thickness (nm)	Composition
Ni128_1	100	20	Ni
NiMg130_2	154	11	$Ni_{0.33}Mg_{0.67}$
NiMg130_3	172	11	$Ni_{0.25}Mg_{0.75}$
NiMg130_4	218	11	$Ni_{0.17}Mg_{0.83}$
NiMg130_5	232	11	$Ni_{0.13}Mg_{0.87}$
NiMg129_3	262	22	$Ni_{0.24}Mg_{0.76}$
Mg131_5	270	10	Mg
Mg152_1	45	10	Mg

Table II. Transition energies (E), integrated areas (A), full width at half maximum (FWHM), branching ratios, $\beta_R = A_3/(A_3+A_2)$, total integrated intensities, (A_3+A_2) and intensity ratios (A_3/A_2) for Ni $L_{3,2}$-edge XRAS of (A) Ni (B & E) $Ni_{0.33}Mg_{0.67}$ (C & F) $Ni_{0.13}Mg_{0.87}$ and (D) Mg_2Ni.

Sample	L_3		L_2		FWHM	β_R	A_3+A_2	(A_3/A_2)
	E_3 (eV)	A_3 (a.u.)	E_2 (eV)	A_2 (a.u.)	(eV)		(a.u.)	
A†	853.5	2.02	870.8	0.66	3.1	0.754	2.68	3.06
B†	853.7	0.88	871.0	0.20	2.0	0.816	1.08	4.40
C†	853.9	1.01	871.1	0.19	2.3	0.840	1.2	5.32
D‡	853.2	1.70	870.3	0.37	3.2	0.821	2.07	4.60
E*	856.0	2.55	873.4	0.81	3.9	0.758	3.36	3.15
F*	856.5	3.07	873.9	0.99	3.6	0.757	4.06	3.10

† XAS measured in transmission mode in He atmosphere.

‡ Total fluorescence yield (TFY) under vacuum.

* XAS measured in transmission mode in 4 % H_2 in He atmosphere.

Table III. Coordination numbers *(N_{Mg})*, bond distances *($R_{Mg\text{-}Mg}$)*, and Debye–Waller factors (σ^2_{Mg-Mg}) obtained from Mg *K*-edge EXAFS for thin films in metallic state.

	Mg-Mg (first shell)			Mg-Mg (second shell)		
Sample	N	R(Å)	σ^2 (10^{-2} Å^2)	N	R(Å)	σ^2 (10^{-2} Å^2)
Mg	12.00(66)	3.203(3)	2.21(19)	4.92(97)	4.568(24)	2.63(19)
$Ni_{0.13}Mg_{0.87}$	8.60(17)	3.098(1)	2.75(7)	2.92(25)	4.465(11)	3.27(7)
$Ni_{0.33}Mg_{0.67}$	3.33(39)	3.038(6)	1.65(35)	1.70(57)	4.472(35)	1.96(35)

Figure Captions

1. Ni $L_{3,2}$-edge transmission mode NEXAFS spectra of thin films measured in He: (a) pure Ni, (b) $Ni_{0.33}Mg_{0.67}$ and (c) $Ni_{0.13}Mg_{0.87}$; in 4 % H_2 in He: (e) $Ni_{0.33}Mg_{0.67}$ and (f) $Ni_{0.13}Mg_{0.87}$. Spectrum (d) Mg_2Ni measured by total fluorescence yield in vacuum. The 6 eV satellite is indicated by arrow. All spectra were normalized to the background. Baselines were shifted for clarity of presentation.

2. Transmission mode Ni $L_{3,2}$-edge NEXAS spectra of $Ni_{0.24}Mg_{0.76}$ thin film measured in He (denoted as 'virgin') and in 4 % H_2 in He (all other curves) as a function of time. The curve denoted as 'end of hydrogenation' was recorded after 24h exposure.

3. Transmission mode Ni $L_{3,2}$-edge NEXAS spectra of $Ni_{0.24}Mg_{0.76}$ thin film in He (solid line), in 4 % H_2 after prolonged hydrogenation (dashed line), and in He after 1 day in air (dotted line).

4. Transmission mode Mg K-edge NEXAFS spectra of thin films in He: (a) Mg, (b) $Ni_{0.13}Mg_{0.87}$, (c) $Ni_{0.33}Mg_{0.67}$; in 4 % H_2 in He: (d) $Ni_{0.13}Mg_{0.87}$ and (e) $Ni_{0.33}Mg_{0.67}$.

5. Mg K-edge NEXAFS spectra of: (a) Mg 270 nm (TFY), (b) Mg 45 nm (transmission in He), (c) Mg_2Ni (TFY), (d) MgH_2 (TFY), and (e) Mg 45 nm (transmission in 4 % H_2 in He).

6. Mg K-edge EXAFS spectra of thin films measured by transmission in He: (a) Mg, (b) $Ni_{0.13}Mg_{0.87}$, (c) $Ni_{0.33}Mg_{0.67}$; in 4 % H_2 in He: (d) $Ni_{0.13}Mg_{0.87}$, (e) $Ni_{0.33}Mg_{0.67}$.

7. Mg K-edge EXAFS spectra of: (a) Mg 270 nm (transmission in He), (b) Mg 45 nm (transmission in He), (c) Mg_2Ni (TFY), (d) MgH_2 (TFY), and (e) Mg 45 nm (transmission in 4 % H_2 in He).

8. Phase corrected and Fourier transformed Mg K-edge EXAFS spectra of Mg, $Ni_{0.13}Mg_{0.87}$, and $Ni_{0.33}Mg_{0.67}$ thin films in the metallic state.

9. Fit results in k space for Mg K-edge EXAFS spectra of Mg, $Ni_{0.13}Mg_{0.87}$ and $Ni_{0.33}Mg_{0.67}$, thin films in the metallic state.

10. Mg K-edge EXAFS in k space for: (a) MgH_2, (b) Mg (45 nm) thin film in hydride state, (c) Mg_2Ni, (d) $Ni_{0.13}Mg_{0.87}$ in hydride state, (e) $Ni_{0.33}Mg_{0.67}$ in hydride, and (f) $Ni_{0.33}Mg_{0.67}$ in metallic state.

Figure 1

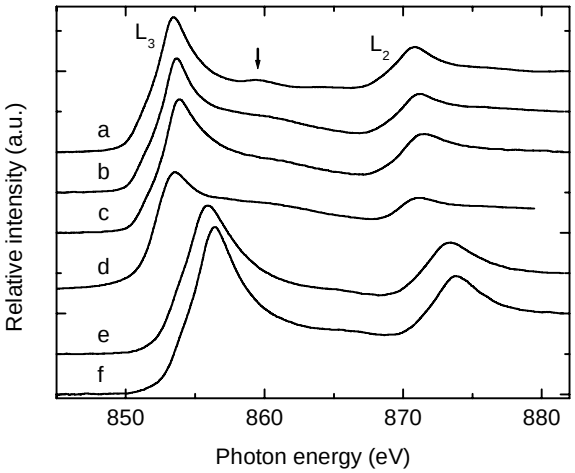
L3
L2
a
b
c
d
e
f
Relative intensity (a.u.)
850
860
870
880
Photon energy (eV)

Figure 2

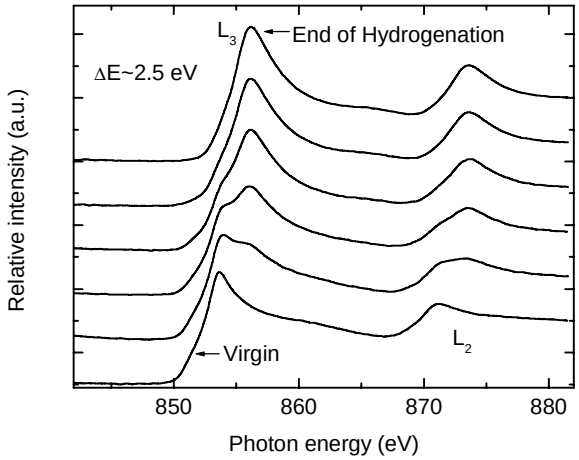
L3
End of Hydrogenation
ΔE~2.5 eV
Relative intensity (a.u.)
Virgin
L2
850
860
870
880
Photon energy (eV)

Figure 3

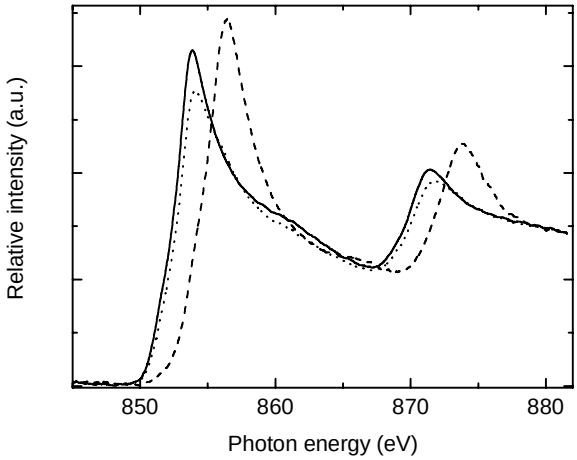

Figure 4

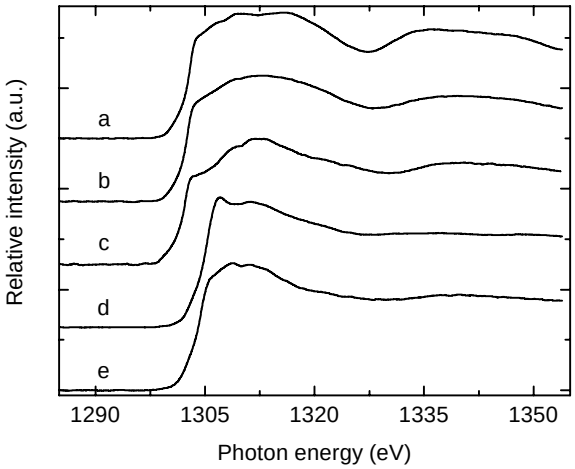
Relative intensity (a.u.)
a
b
c
d
e
1290
1305
1320
1335
1350
Photon energy (eV)

Figure 5

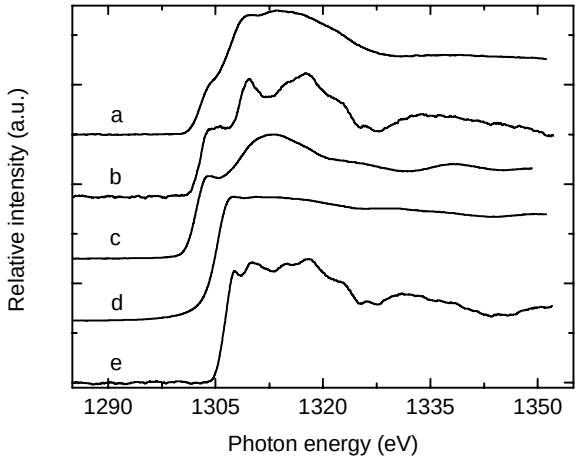
Relative intensity (a.u.)
a
b
c
d
e
1290
1305
1320
1335
1350
Photon energy (eV)

Figure 6

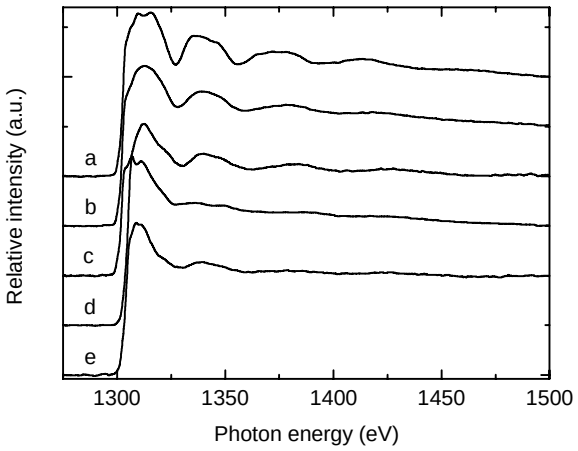
Relative intensity (a.u.)
a
b
c
d
e
1300
1350
1400
1450
1500
Photon energy (eV)

Figure 7

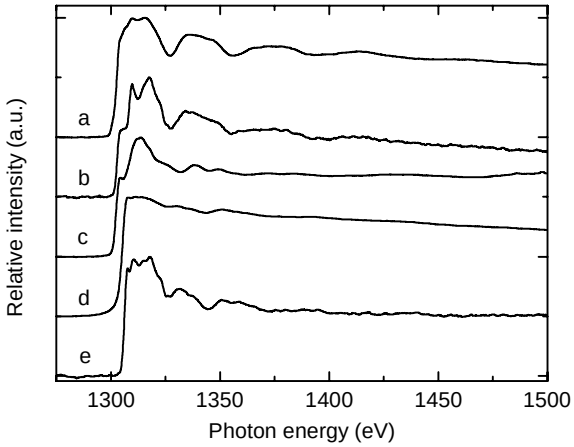
Relative intensity (a.u.)
a
b
c
d
e
1300
1350
1400
1450
1500
Photon energy (eV)

Figure 8

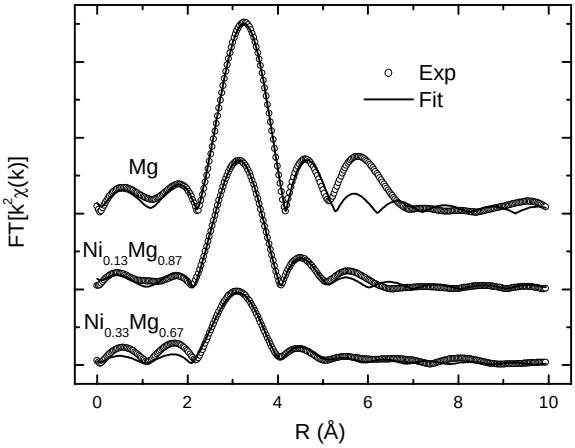

Figure 9

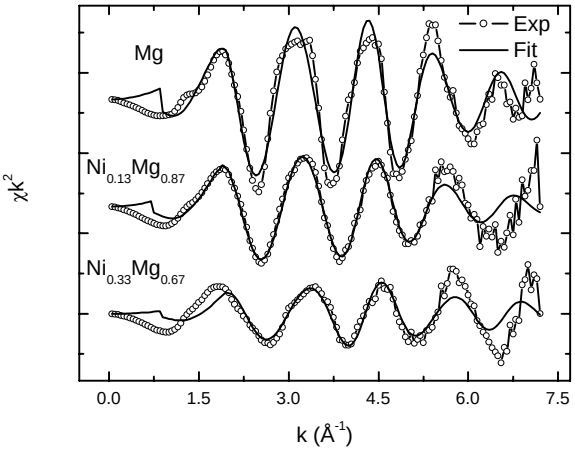

Figure 10